uoka University, Hamamatsu, Japan, in 1980, both in electronic engineering.

He is currently studying towards the Ph.D. degree in electronics at the Research Institute of Electronics, Shizuoka University, Hamamatsu, Japan, where he is primarily involved in microwave solid-state oscillators design and power combining schemes.

Mr. Madihian is a member of the Institute of Electronics and Communication Engineers of Japan.

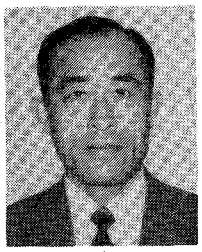

Shizuo Mizushina (S'60–M'66) was born in Hamamatsu, Japan, on August 10, 1933. He received the B. Eng. degree from Shizuoka University, Hamamatsu, in 1957, and the M.Sc. and Ph.D. degrees from Ohio State University, Columbus, in 1962 and 1964, respectively.

From 1957 to 1960 he was a Research Assistant and Lecturer at Shizuoka University. From 1964 to 1965 he was a Member of the Technical Staff at the Bell Telephone Laboratories, Murray Hill, NJ. In 1965 he returned to Shizuoka University where he is a Professor at the Research Institute of Electronics. He has worked on millimeter-wave magnetrons, gigabit-pulse regenerators, solid-state oscillators, and device-circuit interaction problems. His current research interests are concerned with microwave power-combining techniques, microwave thermography, and medical electronics.

Dr. Mizushina is a member of the Institute of Electronics and Communication Engineers of Japan, the Japan Society of Medical Electronics and Biological Engineering, and Sigma Xi.

Simulation Study of Harmonic Oscillators

KLAUS SOLBACH, MEMBER, IEEE

Abstract —**In the last few years, the operating modes of Gunn oscillators for frequencies above 60 GHz have been discussed controversially. In this context, a general theoretical circuit model for oscillators operating in the fundamental and in the second-harmonic modes is studied. The model employs a simple cubic $I-V$ characteristic of the active element and separate embedding circuits for the fundamental and second-harmonic frequencies. The current and voltage waveforms of both modes are contrasted. The oscillator source impedances and the external Q of the second-harmonic mode oscillator are calculated.**

I. Introduction

DURING THE LAST YEARS, several papers have been published concerning the design of second-harmonic GaAs Gunn oscillators for frequencies between 50 and 110 GHz, as well as concerning methods for the classification of existing oscillator designs in terms of the harmonic number [1]–[4]. Indeed, there has been wide unawareness of the possibility of harmonic operation of Gunn oscillators in the past. Such oscillator design as the cap-structure oscillator, used, e.g., by Ondria [5] for GaAs Gunn devices up to frequencies of 110 GHz, exhibited uncommonly high external quality factors Q_e and it was observed that a backshort would have practically very little influence on the oscillator frequency. Attempts were made in the past to explain this unusual behavior by proposing that the Gunn elements were operated in other modes, like the quenched space-charge mode or a hybrid mode.

Barth was one of the first researchers to propose that this behavior would best be explained by assuming the oscillators to be operated as harmonic generation circuits, and he demonstrated this approach to be very efficient in the design of a wide-band-tunable W-band Gunn oscillator [1].

Two experiments have been reported [3], [4], which analyze the harmonic behavior of GaAs Gunn oscillators of the cap type. It is now clear that efficient second-harmonic generation is feasible in the frequency range up to 110 GHz using GaAs Gunn elements and it is reasonable to suspect earlier published oscillator work relied on the same principle.

In this paper, an effort is made to contrast the fundamental circuit behavior of a negative resistance element operated in the fundamental mode with that operated in the second-harmonic mode. A simple nonlinear negative resistance description for the active element is adopted. This $I-V$ characteristic is not a static property of the active element (needs not be valid for dc), but it basically describes that the element at a certain frequency has the ability to generate oscillations (negative resistance) which are limited in amplitude (nonlinearity). Although this description of the element properties is rather general, it has been shown that the fundamental circuit behavior of the fundamental-mode operation of Gunn oscillators may be modeled very well [7]. For Tunnel diodes and one-port-transistor circuits, the model is even more realistic since these elements exhibit static and/or dc current–voltage characteristics very similar to the form employed here.

Manuscript received February 4, 1982; revised April 14, 1982.
The author is with AEG-Telefunken, A1E32, D-7900 Ulm, West Germany.

0018-9480/82/0800-1233$00.75 ©1982 IEEE

II. The Oscillator Model

The model to describe an oscillator, which is capable of fundamental as well as second-harmonic operation, is shown in Fig. 1. The active element is modeled as a real resistance, whose current–voltage dependence is described by a power series

$$I = C_1 V + C_2 V^2 + C_3 V^3. \tag{1}$$

This type of $I-V$ characteristic with $C_2 = 0$ has first been used by van der Pol [6] in his classical work on nonlinear oscillators. The inclusion of the quadratic term $C_2 V^2$ serves to shift the $I-V$ characteristic to an unsymmetric point. The derivation from the otherwise symmetric $I-V$ characteristic is a condition for second-harmonic generation. The magnitude of the quadratic term may be adjusted by an appropriate bias circuitry in physical devices, e.g., Gunn oscillators.

To act as an active source the linear coefficient C_1 has to be a negative number (negative resistance). The cubic term C_3 basically serves to limit the voltages across the element. For example, a typical Gunn element could be described by a negative resistance of about 10 Ω ($C_1 = -0.1$ A/V) and a cubic term C_3 of about 0.01 A/V^3 in order to produce about 166 mW in a fundamental-mode oscillator.

A time-invariant linear network is employed to divide the load impedances into one, which is effective only for the fundamental frequency ω of the oscillation and one effective only for the second-harmonic frequency 2ω.

This frequency-multiplexing network models, e.g., the cap-structure oscillator design, where the cap capacitance together with the bias-post inductance form a quasi-coaxial resonator at the fundamental frequency ω, while at the second harmonic 2ω the cap structure basically acts as a radial transformer to the waveguide.

The aim of this work is to describe the steady-state behavior of the oscillator. It is thus sufficient to employ nodal analysis in the frequency domain, yielding algebraic equations in contrast to nodal analysis in the time domain, yielding integral equations, which are far more difficult to evaluate.

The voltage across the active element is taken to contain only one term for the fundamental and one term for the second-harmonic frequency with all higher harmonics set equal to zero

$$V = V_1 \cdot e^{-j\omega t} + V_2 \cdot e^{-j2\omega t}. \tag{2}$$

The fundamental frequency voltage arbitrarily is set real while the second-harmonic voltage is a complex quantity with the phase φ, $V_2 = V_2 \cdot e^{-j\varphi}$. The physical terminal voltage V relates to the complex quantity via $V = \mathrm{Re}\{V\}$.

Equation (1) is employed to calculate the currents flowing in the circuit when the voltage across the active element is given by (2). It is found that the current flowing into the active element contains a dc component and RF components up to the sixth harmonic

$$I = I_0 + I_1 e^{-j\omega t} + I_2 e^{-j2\omega t} + \cdots + I_6 e^{-j6\omega t}. \tag{3}$$

The direct current I_0 in a practical oscillator has to be

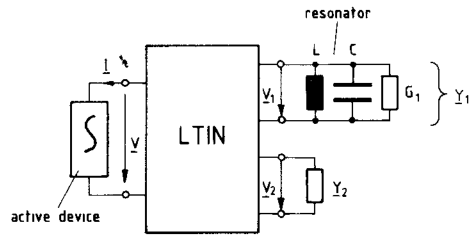

Fig. 1. Equivalent-circuit representation employed to model the oscillator circuit capable of fundamental mode as well as second-harmonic operation.

taken care of by the bias circuit. The first RF current components I_1 and I_2 together with the respective voltages V_1 and V_2 generate power in the fundamental and in the second-harmonic frequencies. The additional higher harmonic currents are not relevant for further analysis since no respective voltage harmonics are allowed in the circuit (2). In this instance currents I_3, I_4, I_5, and I_6 may be properly termed "idler currents."

The first two RF current components readily are calculated as

$$I_1 = C_1 V_1 + C_3\left(\frac{3V_1^3}{4} + \frac{3V_1V_2^2}{2}\right) + C_2 V_1 V_2 \cos\varphi + jC_2 V_1 V_2 \sin\varphi \tag{4}$$

and

$$I_2 = C_1 V_2 + C_3\left(\frac{3V_2^3}{4} + \frac{3V_2V_1^2}{2}\right) + C_2 \frac{V_1^2}{2}\cos\varphi - jC_2 \frac{V_1^2}{2}\sin\varphi. \tag{5}$$

Nodal analysis of the network in Fig. 1 yields two equations for the two frequencies existing in the circuit

$$I_1 + V_1 \cdot Y_1 = 0 \tag{6}$$

and

$$I_2 + V_2 \cdot Y_2 = 0. \tag{7}$$

The evaluation of the nodal equations in connection with the RF currents of (4) and (5) will be treated in the subsequent sections for different modes of operation of the oscillator circuit.

III. Fundamental-Mode Oscillator

The first case to be considered is the conventional fundamental-mode oscillator, which can be formed by letting $Y_2 \to \infty$, i.e., short-circuiting the second-harmonic voltage. With this, only (6) remains to be solved and takes the form of

$$C_1 + C_3 \frac{3V_1^2}{4} + G_1 + j\left(\omega C - \frac{1}{\omega L}\right) = 0. \tag{8}$$

This equation is identical to the original condition for oscillation found by van der Pol.

The frequency of oscillation here is readily found from the condition that the imaginary part $j[\omega C - (1/\omega L)]$ in (8) be vanishing, i.e., $\omega = 1/\sqrt{LC}$, while the real part of (8)

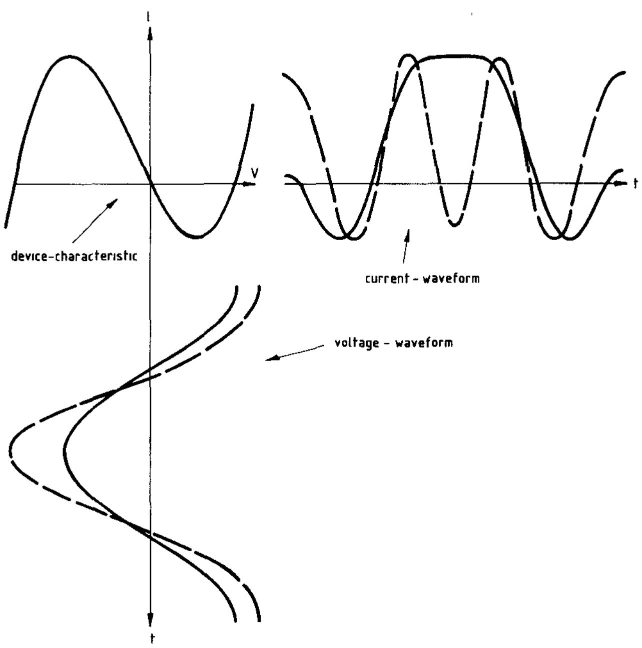

Fig. 2. Device $I-V$ characteristic and current and voltage waveforms for fundamental (—) and harmonic (----) modes of operation. $C_1=-0.1$ A/V, $C_2=0.015$ A/V^2, $C_3=0.01$ A/V^3.

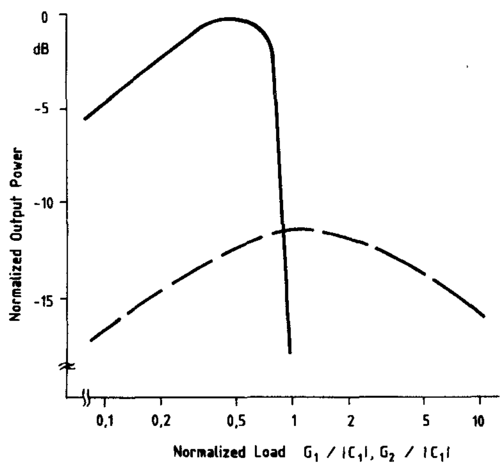

Fig. 3. The output powers of the fundamental- (—) and the harmonic-mode (----) oscillator circuits as a function of the normalized load conductances.

yields the fundamental voltage

$$V_1^2=\frac{4}{3}\left(\frac{-C_1-G_1}{C_3}\right).$$

The current and voltage waveforms of such an oscillation are plotted in Fig. 2 for a special set of coefficients C_1, C_2, and C_3. It can be seen from this plot that although the voltage V is purely cosine shaped, the current I is distorted with respect to the cosine shape. This effect occurs due to the limiting action of the nonlinear active element.

The power output of the oscillator as a function of the load conductance G_1 is plotted in Fig. 3. It is seen that maximum output power is obtained if the load conductance G_1 equals $1/2|C_1|$. For conductances $G_1>|C_1|$ no stable oscillation is possible. The external quality factor for the circuit discussed here is simply the Q of the resonant circuit which forms the load for the fundamental frequency

$$Q_{el}=\frac{Y_0}{G_1},\qquad \text{where } Y_0=\omega C=\frac{1}{\omega L}$$

is the susceptance slope parameter of the resonant circuit.

IV. Harmonic-Mode Oscillator

The second case to be considered is the second-harmonic mode of operation for the oscillator circuit. This mode of operation can be modeled by letting $G_1\to 0$, i.e., no power is dissipated in the fundamental frequency load. This yields two nonlinear, complex equations for the two harmonic voltages V_1 and V_2

$$C_1+C_2V_2\cos\varphi+C_3\left(\frac{3V_1^2}{4}+\frac{3V_2^2}{2}\right)+jC_2V_2\sin\varphi+j\left(\omega C-\frac{1}{\omega L}\right)=0 \quad (9)$$

$$C_1+C_2\frac{V_1^2}{2V_2}\cos\varphi+C_3\left(\frac{3V_2^2}{4}+\frac{3V_1^2}{2}\right)-jC_2\frac{V_1^2}{2V_2}\sin\varphi+Y_2=0. \quad (10)$$

A. Real Harmonic Load Impedance

To facilitate the discussion, it is assumed furthermore that the imaginary part of the second-harmonic load may be set to zero, i.e., $Y_2=G_2$. This implies that $\sin\varphi$ equals zero, since the imaginary part of (10) has to vanish. From $\sin\varphi=0$ in (9), it follows that the imaginary part reduces to the same as in (8), which leads to the same oscillation frequency as in the fundamental-mode oscillator circuit, namely: $\omega=1/\sqrt{LC}$.

At this frequency, the nodal equations reduce to a system of two real, nonlinear equations coupled through the coefficient C_2 of the nonlinear active device $I-V$ characteristic.[1] This system was solved numerically on a computer and for the same set of coefficients C_1, C_2, C_3 as used in the fundamental-mode oscillator case the waveforms of current and voltage at the active element are plotted also in Fig. 2. It can be seen that the voltage waveform swings much further into the nonlinear region of the device $I-V$ characteristic than in the fundamental mode. As a consequence, the current waveform contains much more harmonic-distortion components than in the fundamental mode.

The harmonic output power as a function of the load conductance G_2 is plotted also in Fig. 3. For the set of coefficients used in this example, it can be seen from the graph that the maximum power obtainable from the circuit at the second harmonic is about 11 dB below the maximum power from the fundamental-mode oscillator circuit. It is interesting to note that the maximum power is obtained for $G_2=|C_1|$, that means that the source impedance of the harmonic oscillator circuit is lower than in the fundamen-

[1]This system may be reduced to a single equation of higher degree as well, allowing a simple root-finding algorithm to be used for the solution.

tal-mode circuit. From calculations using various values of C_2 (unsymmetry in the $I-V$ characteristic) it was found that the harmonic power output increases with the value of the coefficient C_2, while in all cases calculated the source impedance was found to be independent of the two coefficients C_2 and C_3. It was found in all cases that the second-harmonic oscillator circuit exhibits a source conductance exactly double that of the fundamental mode circuit.

B. Complex Harmonic Load

If the second-harmonic load is allowed to contain a small imaginary part $Y_2 = G_2 + jB_2$, $B_2 \ll G_2$, the nodal equations split into equations for the real part and for the imaginary part. The imaginary part of (9) becomes

$$C_2 V_2 \sin\varphi + \omega C + \frac{1}{\omega L} = 0 \tag{11}$$

while from (10) it follows that

$$-C_2 \frac{V_1^2}{2V_2} \sin\varphi + B_2 = 0. \tag{12}$$

Since B_2 is supposed to be small: $\varphi \approx 0$ and $\cos\varphi \approx 1$. Thus the real parts of (9) as well as (10) reduce to the same equations as solved in the preceding section, i.e., the amplitudes V_1 and V_2 in this case are the same as in the real load impedance case, Section IV-A.

The phase of voltage V_2 is calculated from (12) as $\sin\varphi = (2V_2/C_2V_1^2)B_2$ and is inserted into (11) to yield

$$2\left(\frac{V_2}{V_1}\right)^2 B_2 + \omega C - \frac{1}{\omega L} = 0. \tag{13}$$

At frequencies near the real load impedance-case resonant frequency $\omega = 1/\sqrt{LC}$ this equation may be written as

$$2\left(\frac{V_2}{V_1}\right)^2 B_2 + 2Y_0\left(\frac{\omega' - \omega}{\omega}\right) = 0. \tag{14}$$

From (14) the oscillation frequency ω' may be calculated, which differs from that of the real load impedance case ω through the effect of B_2. The load-pulling Q-factor (external Q, Q_e) from (14) is readily calculated as

$$Q_{e2} = \frac{Y_0}{2G_2}\left(\frac{V_1}{V_2}\right)^2 \tag{15}$$

which compares to $Q_{e1} = Y_0/G_1$ for the fundamental oscillator mode. It is interesting to note that in both formulas the same susceptance slope parameter appears and that, in the harmonic oscillator case, the external Q-factor increases with the squared ratio of the fundamental and the harmonic components of the active device voltage. Using the results of Section IV-A for the source impedances of both modes of operation it can be shown that for maximum power output in both cases (matched source impedances) the ratio of both Q-factors is then

$$\frac{Q_{e2}}{Q_{e1}} = \frac{1}{4} \cdot \left(\frac{V_1}{V_2}\right)^2. \tag{16}$$

In the harmonic oscillator example plotted in Fig. 2 (dashed line) the ratio of the fundamental and the harmonic voltage components is $V_1/V_2 = 3.71/0.45$, resulting in $Q_{e2}/Q_{e1} = 17$. This means that the pulling quality factor of the harmonic oscillator circuit is more than an order of magnitude higher than in the fundamental oscillator circuit. Furthermore, the analysis of several other calculated examples of harmonic oscillators under different load conditions has led to the conclusion that, in general, the ratio of the Q-factors is only slightly higher than the ratio of the output power from the harmonic oscillator over the power from the load matched fundamental oscillator. In the presented examples the ratio of the output powers under matched conditions is about $P_1/P_2 = -11.3$ dB.

V. Conclusions

Using a specific equivalent-circuit description for an oscillator structure capable of fundamental and second-harmonic operations it was found that the harmonic operation mode has the following features: 1) the harmonic oscillator output power increases with the degree of unsymmetry of the $I-V$ characteristic of the active element (coefficient C_2); 2) the source impedance of the harmonic oscillator is half that of the fundamental oscillator; 3) compared to the fundamental oscillator, the external Q-factor of the harmonic oscillator is increased roughly inversly proportional to the harmonic efficiency, i.e., the output power from the harmonic oscillator over the output power from the load-matched fundamental-mode oscillator.

These theoretical results confirm the observations made in the empirical development of harmonic oscillators using Gunn elements as the active device. In practical oscillators, external Q-factors in the range of 500–1500 are observed when the harmonic efficiencies are in the range of -10 dB [2], [3], [5]. Since the Q-factors of cap-structure oscillators operated in the fundamental mode are generally found on the order of 100 there exists a clear correspondence of the theoretical and the experimental Q-factors of the harmonic oscillator. The exceptionally high Q-factor of 10 000 reported in [1] for the second-harmonic mode as compared to the Q-factor of 45 for the fundamental mode of the oscillator may be explained by the fact that in the specific design the resonator circuit comprises a) the cap structure as employed also in other designs and b) an additional high-Q waveguide resonator. The high-Q waveguide resonator is only effective in the harmonic operation mode, while it is heavily loaded by the output waveguide in the fundamental-mode oscillator version.

With regard to the noise performance of the second-harmonic-mode oscillator it may be stated that the noise-limiting resonator circuit in this mode is much less loaded by the output port than it is in the fundamental mode of operation. Thus the noise power produced in the oscillator is less than that in the fundamental-mode oscillator.

This topic has not been investigated theoretically, but experimental second-harmonic Gunn oscillators have been reported to show noise performances about 3 dB better than fundamental-mode oscillators using the same Gunn element.

References

[1] H. Barth, "A wideband, backshort-tunable second harmonic W-band Gunn-oscillator," in *1981 IEE-MTT-S Int. Microwave Symp. Dig.*, pp. 334–337.

[2] M. J. Lazarus, F. R. Pantoja, S. Novak, and M. G. Somekh, "Wide-band tunable mm-wave Gunn oscillator design," *Electron. Lett.*, vol. 17., no. 20, pp. 739–741, Oct. 1981.

[3] I. G. Eddison and D. M. Brookbanks, "Operating modes of millimeter wave transferred electron oscillators," *Electron. Lett.*, vol. 17, no. 3, pp. 112–113, Feb. 1981.

[4] W. H. Haydl, "Harmonic operation of GaAs millimeter wave transferred electron oscillators," *Electron. Lett.*, vol. 17, no. 22, pp. 825–826, Oct. 1981.

[5] J. Ondria, "Wide-band mechanically tunable W-band (75-110 GHz) CW Gunn diode oscillator," presented at the AGARD-Conf. Millimeter and Submillimeter Wave *Propagation and Circuits*, (München/FRG), Sept. 1978, Conf. Reprint no. 245, pp. 12-1–12-16.

[6] B. van der Pol, "The nonlinear theory of electric oscillations," *Proc. IRE.*, vol. 22, pp. 1051–1086, 1934.

[7] M. Bischoff, "Ein Verfahren zur Optimierung von Millimeterwellen-Gunnoszillatoren aus dem Ersatzschaltbild," *Arch. Nachrichtentech. der ntz* (Germany), vol. 7, pp. 161–164, 1979.

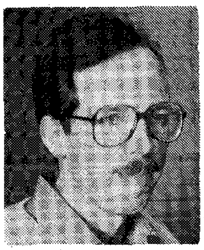

Klaus Solbach (M'80) was born in Witten, West Germany in 1951. He recieved the Dipl.-Ing. degree from the Technical University of Aachen, West Germany, in 1974 and the Dr.-Ing. degree from the University of Duisburg, West Germany, in 1979.

From 1975 to 1980 he had been employed at the University of Duisburg as a Research Assistant. He has been engaged in investigations of the properties and circuit applications of dielectric image lines in the millimeter-wave frequency range.

In 1981 he joined AEG-Telefunken in Ulm, West Germany, where he is engaged in the development of integrated millimeter-wave circuits.

A Waveguide-Cavity Multiple-Device FET Oscillator

ANDRZEJ MATERKA AND SHIZUO MIZUSHINA, MEMBER, IEEE

***Abstract*—A waveguide-cavity oscillator, applicable to power-combining circuits, has been developed using probe for coupling between active device and cavity. No lossy stabilizing element is required. The control of output power, oscillation frequency, and injection locking bandwidth are performed easily. Output power of 44 mW and dc-RF conversion efficiency of 33.2 percent were obtained at 9.2 GHz for a single-device low-power FET oscillator. A simple technique of cascading the pretuned oscillator modules was used to construct multiple-device oscillators incorporating up to four FET's with combining efficiency of about 100 percent.**

I. Introduction

Gallium arsenide FET's offer attractive performance as microwave power sources, especially because of their efficiency and output power capabilities which have been steadily improving for the last few years [1]. For further increase of the output power from FET amplifiers several combining techniques have been developed [2]; however, no work has been reported on adding the power from FET oscillators. In the present paper, a waveguide-cavity oscillator is described which can be used to combine power from individual FET devices with high efficiency.

Manuscript received December 4, 1981; revised March 8, 1982.

A. Materka is with the Research Institute of Electronics, Shizuoka University, Hamamatsu 432, Japan, on leave from the Institute of Electronics, Lodz Technical University, Lodz, Poland.

S. Mizushina is with the Research Institute of Electronics, Shizuoka University, Hamamatsu 432, Japan.

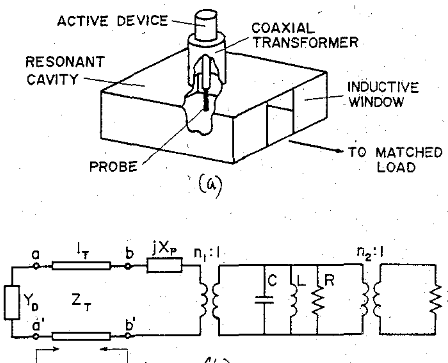

Fig. 1. (a) A waveguide-cavity single-device oscillator and (b) its equivalent circuit.

II. Description and Analysis

Fig. 1(a) shows a single-device oscillator of the proposed type in which an active device is placed at one end of a coaxial transformer. The other end of the transformer is coupled to the cavity by a probe. The cavity in turn is coupled to the matched waveguide through an inductive window. An equivalent circuit of the oscillator, for frequencies close to the cavity dominant resonant frequency, is shown in Fig. 1(b). The active device is represented by a